Journal of Fluid Science and Technology

Vol. 6, No. 3, 2011

Preliminary Study on the Optimum Design of a Tension Leg Platform for Offshore Wind Turbine Systems*

Kenji SHIMADA**, Masahiro MIYAKAWA**, Takumi OHYAMA**,
Takeshi ISHIHARA***, Yukinari FUKUMOTO****,
Kouichirou ANNO*****, Hideaki OKADA***** and Yoichi MORIYA*****

** Shimizu Corporation,
1-2-3 Shibaura, Minato-ku, Tokyo 105-8007, Japan
E-mail: shimaken@shimz.co.jp
*** The University of Tokyo,
7-3-1, Hongou, Bunkyo-ku, Tokyo 113-8656, Japan
**** Tokyo Electric Power Company,
4-1, Egasaki-cho, Tsurumi-ku, Yokohama, Kanagawa 230-8510, Japan
***** Penta-Ocean Construction CO., LTD.,
2-2-8, Koraku, Bunkyo-ku, Tokyo 112-8576, Japan

Abstract

We demonstrate a procedure for determining the configuration of a tension leg platform (TLP) on which a 2.4 MW wind turbine can be installed. Various sizes of the structural elements of the TLP are examined to investigate their effects on tendon tension and response acceleration at the top of the tower. It is shown that although increasing the volume of the peripheral column reduces the acceleration response, it amplifies the tendon tension, while increasing the span length between the center and peripheral columns reduces both of them. Furthermore, the relevant determination of the initial tension is investigated.

Key words: Offshore Wind Energy, Tension Leg Platform, Initial Tension, Acceleration, Displacement, Tendon

1. Introduction

We have developed semisubmersible-type floating structures for offshore wind turbine systems[(1)(2)]. These structures have shown good performance as base floaters for offshore wind turbine systems. A variety that is suitable for wind turbine systems is the tension leg platform (TLP)[(3)(4)]. Because the TLP exhibits moderate wave-induced motion, especially for roll and pitch, it can be considered its dynamic characteristics accommodate to install an onshore wind turbine with minimum modification. Among the parameters involved in the design of a TLP, relevant initial tension must be imposed to prevent the loosening of tension in its tendons, which causes impact stress due to snap loading. Here we present an initial determination methodology for the optimum configuration of a TLP for an offshore wind turbine that satisfies the requirements of both structural safety under storm conditions and serviceability under cut-out wind conditions.

2. Structure of the TLP

Figures 1 and 2 show a model of a TLP. Its structure resists external excitations with three tendon legs, each consisting of double high-strength steel cables (cross-sectional area

*Received 1 Nov., 2010 (No. 10-0505)
[DOI: 10.1299/jfst.6.382]

of a cable A = 9270 mm^2, Young's Modulus E = 196 kN/mm^2, failure load per cable T_f = 14,600 kN[4]). A 2.4 MW wind turbine is assumed to be installed on the TLP. The weight of the wind turbine is 300 t and the depth of the construction site is assumed to be 100 m. Because this structural configuration may be a minimal compact configuration, it may be worth investigating in detail.

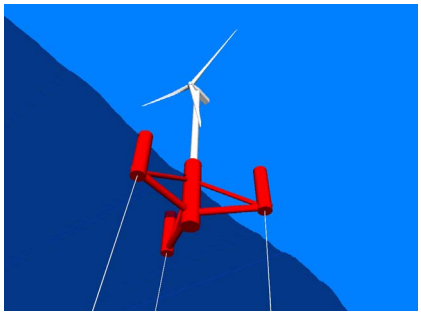

Fig. 1 Configuration of the TLP.

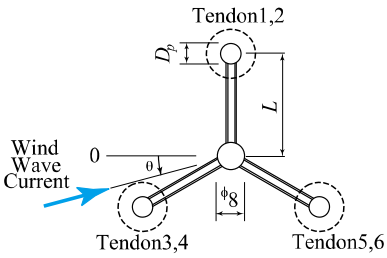

(a) Plan view

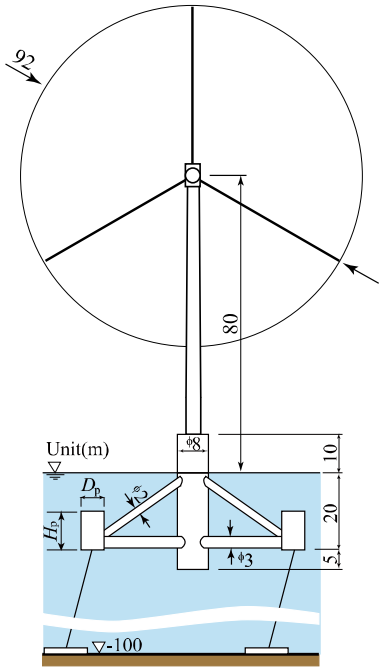

(b) Elevation

Fig. 2 Parameters used in this study.

3. Analytical Method

The numerical model is based on the combination of Morison forces and diffraction forces by McCamy-Fuchs[5] and is solved in the frequency domain. As the effect of the drag force on the member of the TLP is dominant, the drag force is incorporated by reflecting its nonlinear effect in a linearized manner[1]. The external forces are assumed to be collinear wind, waves, and current, where the maximum wind and mean current loads are modeled as steady forces. Values of the maximum wind load acting on the wind turbine were supplied by the manufacturer.

The TLP is modeled as a rigid body having six degrees of freedom, with the moorings represented as translational linear springs. In this analysis, the moorings are assumed to be taut and the effects of the current and wave forces on them are neglected.

Determination of the tendon tension is illustrated in Fig. 3. At the beginning of the analysis, the TLP is balanced with initial tension T_0 in an initial hydrostatic equilibrium position. Next, a steady-state equilibrium position where the floating body is balanced with the steady forces is determined and the consequent tendon tension in the position is defined as the steady tension T_{steady}. Finally, the maximum and minimum tendon tensions in a dynamic equilibrium state are approximated as follows:

$$\begin{cases} T_{\max} \approx T_{steady} + \alpha T_{1/3} \\ T_{\min} \approx T_{steady} - \alpha T_{1/3} \end{cases} \quad (1)$$

where $T_{1/3}$ is the significant value of the tendon tension = $2\sigma_T$. σ_T is the standard deviation of the dynamic tension T, which is calculated following linearized tension as

$$T \approx k\left(n_x \Delta x + n_y \Delta y + n_z \Delta z\right) \tag{2}$$

where k is the stiffness of the tendon $k = EA/l_0$; l_0 is initial length of a tendon; (n_x, n_y, n_z) are the directional cosines at the steady-state balanced position; and $(\Delta x, \Delta y, \Delta z)$ are the displacements, which are the deviations from the steady-state balanced position. α is the ratio of the most frequent value of the maximum tension to its significant value, which is discussed in section 4.1.

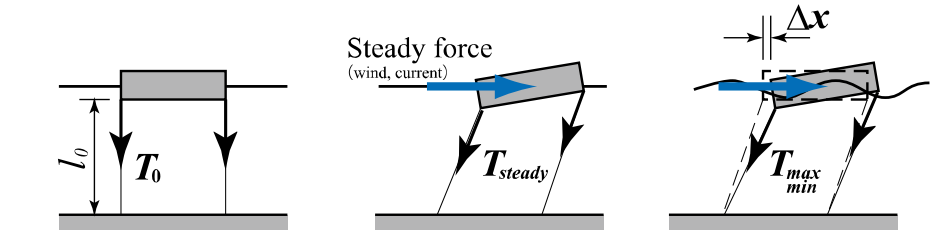

Fig. 3 Definition of tendon tension at each equilibrium state.

If the minimum tension is less than zero, the tendon is in a state of slack. When the tendon is returning to taut from being slack, a large snap impact load occurs. To avoid this situation, a certain amount of initial tension must be appropriately introduced.

The TLP is assumed to be located in a region several kilometers offshore in the Pacific Ocean of Japan. Table 1 shows the wind turbine and metocean conditions. Irregular wave motions are analyzed in the calculation by assigning the Bretschneider-Mitsuyasu[6] wave spectrum (Fig. 4).

Table 1. Wind turbine and metocean conditions.

Wind conditions	Design situation	Wind (m/s)	Significant wave height (m)	Wave period (s)	Current (m/s)
Rated	Power production	12.5	3.9	7.4	1.85
Cut-out	Parked	25.0	7.1	9.8	
Storm (50-year)	Parked	50.0	12.0	13.4	

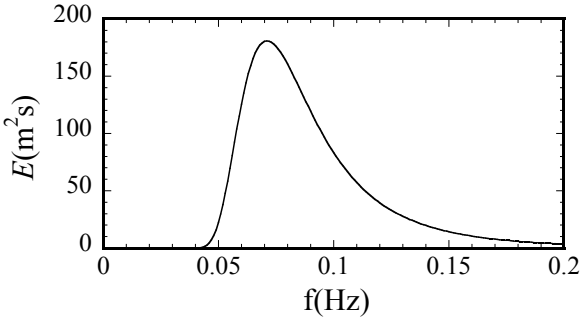

Fig. 4 Bretschneider-Mitsuyasu spectrum under storm conditions.

4. Results

4.1 Dynamic characteristics of TLP

In Fig. 5, the frequency response functions of the TLP model are illustrated for sway, heave, and roll motions. The peak response for each direction was found to have been successfully designed to be located far beyond the significant wave period where a large content of wave energy is included. Furthermore, the peaks become broader as wind speed increases due to the damping that arises from drag forces.

Because the natural periods of the TLP are longer than the significant wave period, the

motion of the TLP will be compliant to wave motion. Thus, dynamic tension can also be assumed to be compliant to wave motion. According to the Rayleigh distribution, $\alpha = 1.8$ corresponds to the ratio of the most frequent value of the maximum value to the significant value during approximately 3 h.

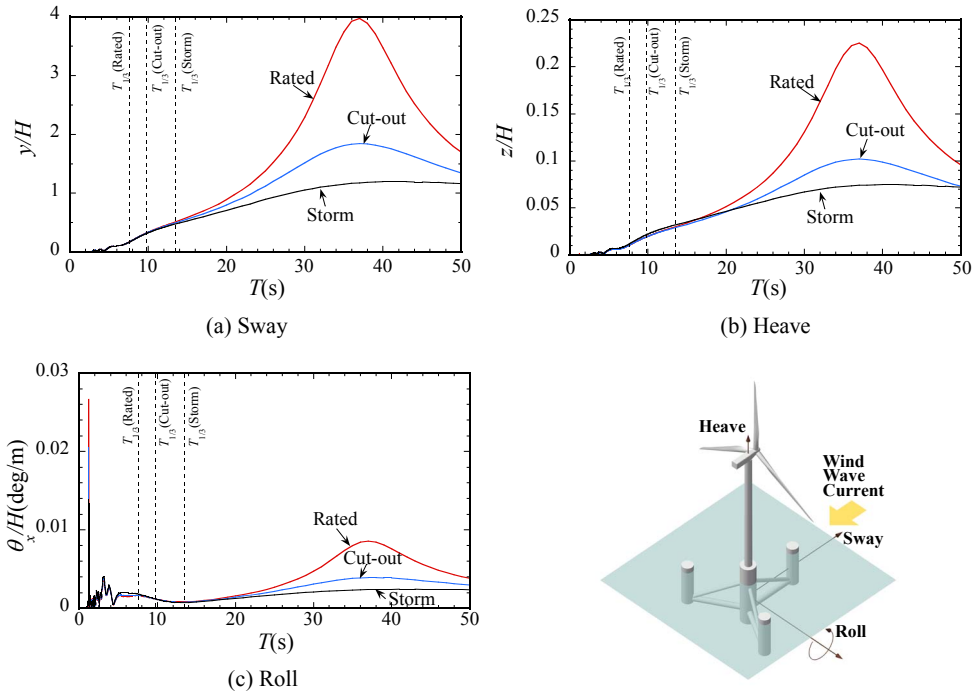

Fig. 5 Frequency response functions of the TLP (L:D_p:H_p = 30 m: 6 m: 23 m; T_0 = 2290 kN).

4.2 Variation of tension in a tendon with the direction of forces

Tension in a tendon varies with the direction of the external forces. Figure 6 shows the tension variation for tendon No. 1 against wind direction with the other forces in various combinations (Table 2). For all cases listed in Table 2, the maximum tension occurs at θ = –90°, whereas the minimum occurs at θ = +90°. As the values of the other tendons are identical to this in point symmetry with an angle of ±120°, the following studies are represented by tendon No. 1.

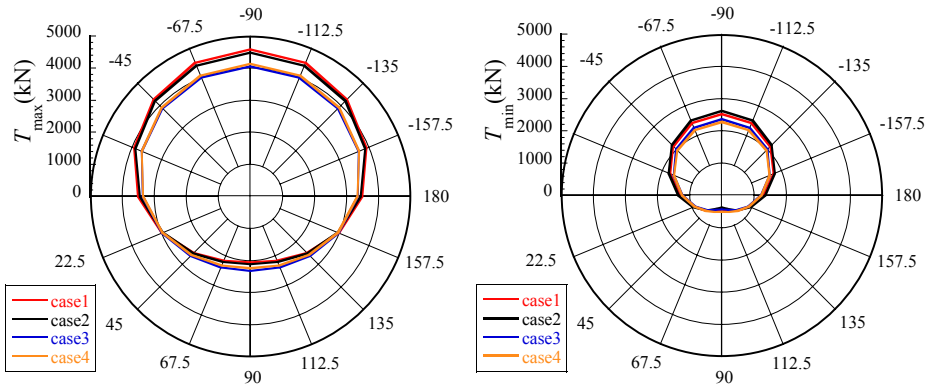

Fig. 6 Tensions in tendon No. 1 for wind direction θ (L:D_p:H_p = 30 m: 6 m: 23 m; T_0 = 2290 kN under storm conditions).

Table 2. Combination of wind, wave, and current directions.

Case		Wind	Current	Wave
1	Collinear	○	○	○
2	Wave adverse	○	○	●
3	Wave and current adverse	○	●	●
4	Current adverse	○	●	○

○ : collinear to wind, ● : adverse to wind

4.3 Determination of initial tension

Figure 7 demonstrates the dependencies of the maximum and minimum tensions on the initial tension T_0. In the figure, the abscissa demonstrates initial tension as ΣT_0/displacement which expresses a ratio of sum of them to displacement of the TLP. In this figure, only two representative lines that correspond to wind directions $\theta = -90°$ and $+90°$ are shown as the lines for the other wind directions are bounded by these two lines. Both of them are nearly proportional to the displacement and are parallel to the initial tension, which is expressed by the inclined dashed line in the figure, i.e., the dynamic component of the tensions has little dependence on the initial tension.

Hence, to design a tendon to ensure its safety for all directions, i.e., to prevent a cable failure from either maximum load or a loosening of tension, an initial tension T_0 should be introduced where $T_{0\min} \le T_0 \le T_{0\max}$. Here, $T_{0\max}$ and $T_{0\min}$ are initial tensions for which the maximum line coincides with T_f/γ_s and the minimum line coincides with zero tension, respectively, where γ_s is a safety factor for the failure load of a tendon. In DNV-OS-E301[7], a partial safety factor for the moorings under the ultimate limit state condition, 2.5 is specified. In this study, γ_s =3 is assumed. In the figure, the shaded area is the design-possible area with the following condition:

$$T_{0_{\min}} \le T_{0_{\max}} \tag{3}$$

That is, the initial tension cannot be specified arbitrarily. If a combination of L, D_p, and H_p fulfils this condition, where D_p and H_p are the diameter and height of the peripheral column, respectively, and L is the distance between the central and peripheral columns (see Fig. 2), a design situation that is based on this selection is structurally valid. In this example, the possible initial tension is limited to within 30% to 40% of the displacement of a floating body. If the tension is further amplified, this area becomes narrower and ultimately vanishes. In such a case, the relevant strength of the tendon cable, i.e., a higher-grade cable, should be selected. This, however, would be achieved with a trade-off in cost.

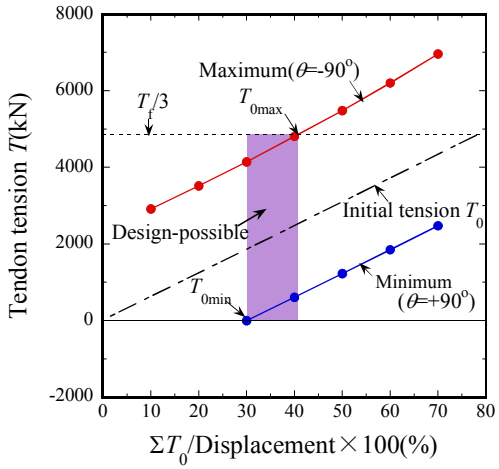

Fig. 7 The maximum and minimum tendon tension dependencies on the initial tension and a design-possible area (L:D_p:H_p = 30 m: 6 m: 23 m, tendon No. 1, under storm conditions).

4.4 Effect of the configuration of the TLP on the tension

Next, the effect of the dimensions of the structural elements, i.e., D_p, H_p, and L, on the tendon tension is investigated. Here, the draft is kept constant. From Figs. 8 and 9, the maximum (minimum) tension increases (decreases) with increasing D_p and H_p. Meanwhile, from Fig. 10, they decrease (increase) with increasing L. That is, an increase in volume of the peripheral column as well as a decrease in the span length leads T_{0max}–T_{0min} to decrease, limiting the possible choice of the initial tension.

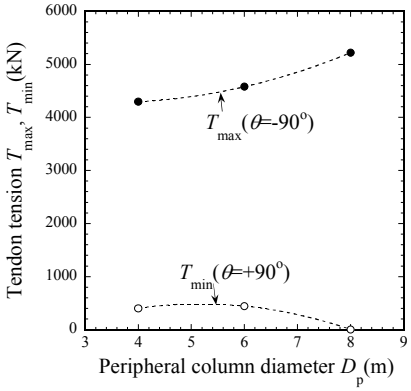

Fig. 8 Tendon tension dependency on D_p (L:H_p = 30 m: 23 m, T_0 = 2290 kN, under storm conditions).

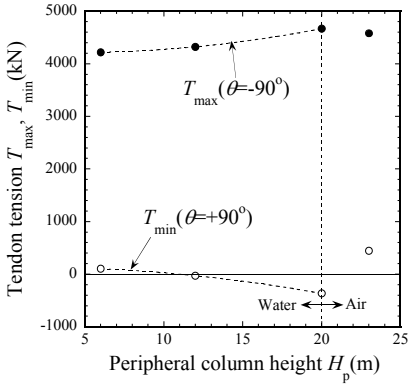

Fig. 9 Tendon tension dependency on H_p (L:D_p = 30 m: 6 m, T_0 = 2290 kN, under storm conditions).

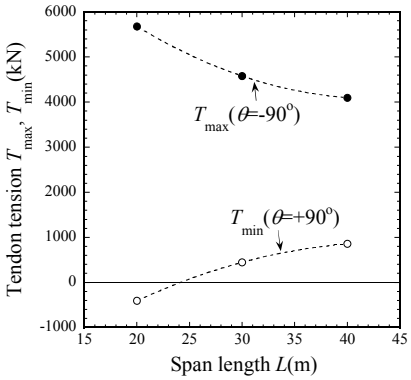

Fig. 10 Tendon tension dependency on L (D_p:H_p = 6 m: 23 m, T_0 = 2290 kN, under storm conditions).

4.5 Acceleration at the cut-out wind speed

Using the above procedure, the 27 combinations listed in Table 3 were examined. It was found that no combination that includes L = 20 m is design possible. Even L = 30 m, No. 18, in which D_p and H_p are the largest among the combinations, is not design possible.

For the remaining 17 design-possible cases, an initial tension was specified equal to the mid-value of the design-possible area, i.e., $T_0 = (T_{0max} + T_{0min})/2$, as listed in Table 3. However, in this study, since a safety factor of γ_s = 3 is already considered for the upper bound of the tension, it may also be reasonable to set the initial tension at the larger side of the design-possible area, i.e., $T_0 = T_{0max}$, in order to achieve a larger margin for the lower bound.

Finally, among the selected candidates, combinations that satisfied the allowable horizontal acceleration of 0.2 G [8] were chosen as the final selections that provide for both structural safety and serviceability. Figure 11 to 13 plot the maximum acceleration at the top of the tower (at hub height) which is defined as 1.8 times the significant value of the acceleration. Acceleration was found to decrease with an increase in any of D_p, H_p, or L. In

Fig. 14, the maximum accelerations are plotted against the displacement of the TLP. A trade-off between the acceleration and displacement is observed in which low acceleration needs large displacement, which might be in proportion to the cost of the structure. In Fig. 15, the total initial tension is shown as a function of displacement. The range of possible initial tensions is from 34% to 50% for L = 30 m and from 23% to 55% for L = 40 m, thus it is found to become wider with increasing span length.

In Fig.15, results are classified into two groups, i.e. H_p=6, 12m and H_p =23m, where the peripheral columns of the former are submersible whereas the latter is semi-submersible. From the regression lines for these groups, it can be concluded that regardless of the size of the span length and diameter of the peripheral column, T_0=2548(kN) and T_0=2279 (kN) are reasonable estimates for the TLP with submersible peripheral columns and semi-submersible columns, respectively.

Table 3. Structural parameters and the maximum acceleration at hub height

TLP No.	L (m)	D_p (m)	H_p (m)	Disp. (t)	T_0 (kN)	ΣT_0/Displacement (%)	Maximum acceleration (m/s^2)
1	20	4	6	2099.3	-	-	-
2	20	4	12	2242.3	-	-	-
3	20	4	23	2552.9	-	-	-
4	20	6	6	2266.1	-	-	-
5	20	6	12	2790.3	-	-	-
6	20	6	23	3489.2	-	-	-
7	20	8	6	2639.4	-	-	-
8	20	8	12	3571.3	-	-	-
9	20	8	23	4813.9	-	-	-
10	30	4	6	2317.4	2500	66.0	2.533
11	30	4	12	2550.4	2500	60.0	2.232
12	30	4	23	2861.0	2300	49.2	1.906
13	30	6	6	2575.7	2500	59.4	2.185
14	30	6	12	3099.9	2500	49.4	1.804
15	30	6	23	3798.9	2150	34.7	1.553
16	30	8	6	2950.5	2500	51.9	1.854
17	30	8	12	3882.4	2600	41.0	1.524
18	30	8	23	5125.0	-	-	-
19	40	4	6	2627.0	2500	58.3	2.165
20	40	4	12	2860.0	2550	54.6	1.930
21	40	4	23	3170.6	2350	45.4	1.644
22	40	6	6	2885.9	2500	53.0	1.881
23	40	6	12	3410.1	2600	46.7	1.569
24	40	6	23	4109.0	2200	32.8	1.348
25	40	8	6	3261.2	2600	48.8	1.632
26	40	8	12	4193.2	2600	38.0	1.297
27	40	8	23	5435.7	2050	23.1	1.235

1) Here, cases shaded by satisfy the acceleration response criterion.
2) As cases 1-9 and 18 are design-impossible, T_0 and the maximum accelerations are not calculated.

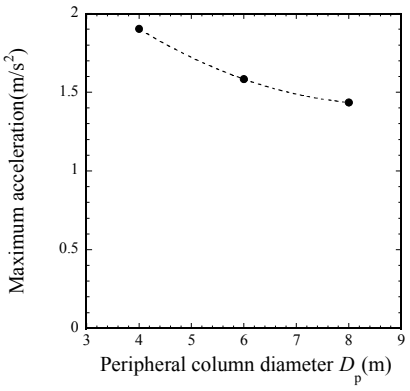

Fig. 11 Hub height maximum acceleration dependency on D_p (L:H_p = 30 m: 23 m, T_0 = 2290 kN, under cut-out wind speed conditions, –90°).

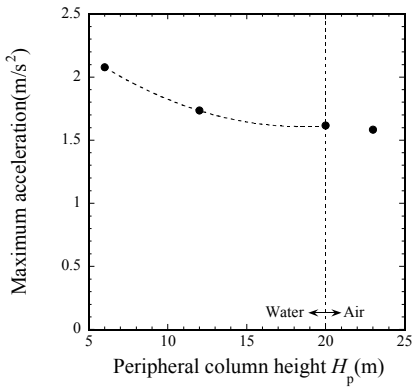

Fig. 12 Hub height maximum acceleration dependency on H_p (L:D_p = 30 m: 6 m, T_0 = 2290 kN, under cut-out wind speed conditions, –90°).

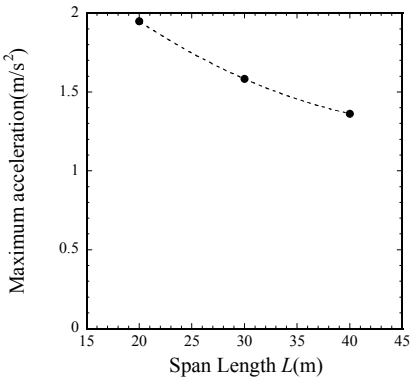

Fig. 13 Hub height maximum acceleration dependency on L (D_p:H_p = 6 m: 23 m, T_0 = 2290 kN, under cut-out wind speed conditions, –90°).

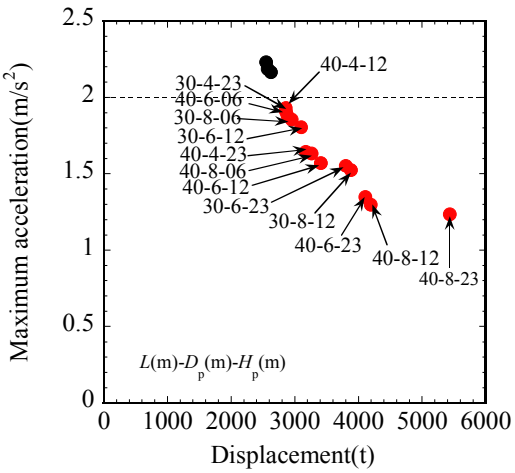

Fig. 14 The maximum horizontal accelerations at hub height under cut-out wind speed conditions and displacements of final selected candidates.

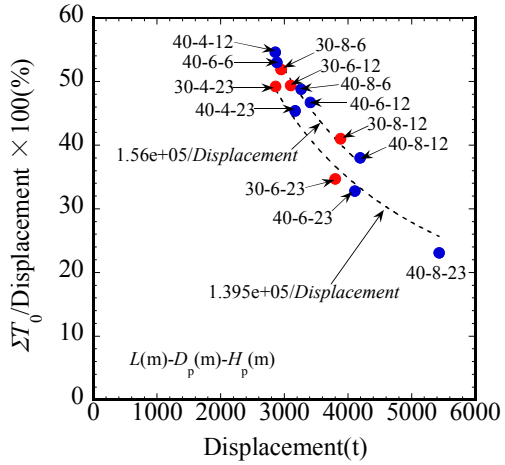

Fig. 15 Relationship between displacement and total initial tension.

5. Conclusions

A preliminary study toward the optimum design of a TLP for an offshore wind turbine was performed primarily with respect to the determination of the initial tension and configuration. The main findings are summarized as follows:

(1) Tendon tension becomes maximum at a wind direction of –90° and minimum at +90° when the wind, waves, and current are collinear.

(2) Possible choice of the initial tension extends with decreasing volume of the peripheral column, and with increasing span length between the center and peripheral columns.

(3) The maximum acceleration at hub height decreases with any increase in the volume of the peripheral column or in the span length between the center and peripheral columns.

Nomenclature

A : cable cross-sectional area
D_p : peripheral column diameter
E : Young's Modulus
L : distance between the central and peripheral columns
l_0 : initial length of a tendon
H : wave height
H_p : peripheral column height
k : tendon stiffness, $k = EA/l_0$
n_x, n_y, n_z : directional cosines at the steady-state balanced position
T : dynamic tension
T_f : failure load per cable
T_{max} : maximum tension
T_{min} : minimum tension
T_{steady} : steady tension
T_0 : initial tension
$T_{1/3}$: significant value of the tendon tension = $2\sigma_T$
T_{0max} : upper limit of initial tension
T_{0min} : lower limit of initial tension
y : sway displacement
z : heave displacement
Δx, Δy, Δz : displacements that are deviations from the steady-state balanced position
α : ratio of the most frequent value of the maximum tension to its significant value
γ_s : safety factor for failure load of a tendon
θ : direction
θ_x : roll displacement
σ_T : standard deviation of the dynamic tension T

References

(1) Shimada, K. et al., A Study on a Semi-Submersible Floating Offshore Wind Energy Conversion System, *Proc. of the 17th International Offshore and Polar Engineering Conference* (2007), 2007-NM-02.
(2) Shimada, K. et al., Structural Optimization and Verification of Economical Scale Merit on a Semi-Submersible Floating Offshore Wind Energy Conversion System, *21st Ocean Engineering Symposium* (2009-8), OES21-13.
(3) Fulton, G.R. et al., Semi-Submersible Platform and Anchor Foundation Systems for Wind Turbine Support, NREL/SR-500-40282 (2007).
(4) Suzuki, K. et al., Initial Design of TLP for Offshore Wind Farm, *Proc. of Renewable Energy 2010 International Conference* (2010), O-Wd-9-5.
(5) McCamy, R. and Fuchs, R., Wave forces on piles : a diffraction theory, Tech Memo No.69,

(Beach Erosion Board, U.S. Army Corps of Engineers, Washington DC) (1954).

(6) Mitsuyasu, H., On the growth of spectrum of wind-generated waves (2) – spectral shapes of wind waves at finite fetch –, *Proc. 17th Japanese Conf. on Coastal Engineering*. (1970), pp. 1-7 (in Japanese).

(7) DNV-OS-E301 Position Mooring (2010), p. 45.

(8) Fukumoto, Y. et al., A Study of Floating Offshore Wind Turbine Systems (Part III) Investigation of Reinforced Concrete Spar-Buoy for Offshore Wind Turbine, *Proc. of the 28th Wind Energy Symposium* (2006), pp. 204-207.